Dissolution Kinetics of Iron Containing Materials in Sour Wells*

Jun Ma[1,2], Tihana Fuss[1], Jingyu Shi[1], and Juanying Liu[2]

Search and Discovery Article #41638 (2015)
Posted June 30, 2015

*Adapted from extended abstract prepared in conjunction with poster presentation at AAPG Annual Convention & Exhibition 2015, Denver, Colorado, May 31-June 3, 2015.

[1]Saint-Gobain Proppants, Stow, Ohio, United States (tihana.fuss@saint-gobain.com)
[2]Saint-Gobain Research (Shanghai), Shanghai, PR China

Abstract

Crude oil and natural gas can carry various high-impurity products, which are inherently corrosive, such as, carbon dioxide (CO_2) and hydrogen sulfide (H_2S). These impurities increase operational safety risks and can be detrimental to production, both in terms of equipment damage and permeability impairment caused by scale deposition. Problems with iron sulfide scale occur when H_2S comes in contact with spent acid solutions containing dissolved iron ions. While dissolution of pipe and iron bearing core materials in H_2S solutions is known to result in FeS scale deposition, the reactivity of iron containing proppant material under sour conditions is poorly understood and with little documentation.

The present study evaluates and compares dissolution kinetics of iron bearing formation and iron containing proppants in an H_2S acid solution in order to evaluate their relative contributions to iron sulfide scale deposition. The study uses X-ray diffraction (XRD) and inductively coupled plasma optical emission spectroscopy (ICP-OES) analysis to qualify Fe containing crystallite forms and quantify dissolution and scale build up reaction kinetics. Scanning Electron Microscopy (SEM) is used to evaluate surface morphology changes associated with iron dissolution and iron sulfide scale deposition. Finally, reactivity of all tested materials is compared based on their initial iron concentration and relative dissolution affinity.

Introduction

Utilization of fracturing methods allows economical extraction of oil and gas resources from unconventional plays. Development of unconventional resources increases proppant consumption resulting in a high increase for proppant used per well site. With this sharp increase in proppant volume environmental and chemical stability of current proppant solutions require extra evaluation.

Crude oil and natural gas fluids often carry various inherently corrosive substances, such as carbon dioxide (CO_2), hydrogen sulfide (H_2S), and free water (Lusk et al., 2008). These impurities increase operational safety risks and can be detrimental to production, both in terms of equipment damage and permeability impairment caused by scale deposition.

Issues concerning operational safety revolve around the handling of H_2S compounds and vapors at well sites. Documented studies show eight-hour exposure to concentrations greater than 100 ppm H_2S can cause hemorrhage and death (Tuttle, 1987). H_2S compounds can also negatively affect the wells' economic performance by both impacting wells' cumulative production and the economic value of the produced hydrocarbons.

Presence of CO_2, H_2S, and free water in producing fluids can cause equipment corrosion and failure, exposing an operator to an environmental and ecological risk and large clean up fees (Oyelami and Asere, 2011). Corrosion of steel pipes is of greatest concern and is influenced by temperature, CO_2 and H_2S content, water chemistry, flow velocity, and surface conditions (Nalli, 2010).

Furthermore, the impurities (CO_2, H_2S, and free water) can be detrimental to oil/natural gas production in terms of permeability and productivity loss caused by scale deposition. Problems with iron sulfide scale occur when H_2S encounters dissolved iron ions (Nasr-EI-Din and AI-Humaidan, 2001). FeS scale deposition caused by a reaction between H_2S and steel pipeline walls and/or iron bearing core materials is a known industry problem. Today the most common approach used to minimize FeS scale deposition risk is addition of H_2S scavengers (Nasr-EI-Din et al., 2000a; Nasr-EI-Din et al., 2000b; Nasr-EI-Din et al., 2000c; Nasr-EI-Din et al., 2007; Leal et al., 2007), as well as, minimization and control of the use of iron bearing compounds during well completion.

Ceramic proppant are engineered materials typically manufactured from either clay (kaolin) or bauxite raw minerals. Each of these minerals occupies a unique regime in the Al_2O_2-SiO_2 system: bauxite minerals contain more than 60 wt.% Al_2O_2 while clay minerals contain less than 45% wt.% of Al_2O_2. High temperature thermal processing of kaolin and bauxite materials, also known as sintering, converts these minerals into their high temperature crystalline forms. Proppants made from these minerals consist of two major phases: corundum and mullite. As clay based proppants have excess of silica, high temperature processing results in formation of crystalline and amorphous silica compounds. On the other hand, bauxite based proppants contain various levels of iron, most typically between 1-10 wt.%. During high temperature processing, required to sinter proppants, iron in these bauxite minerals forms pseudobrookite, a high temperature iron aluminate phase.

During hydraulic fracturing, high volumes of bauxite-based ceramics are injected and placed in the fractures. These proppants remain in the formation for the - life of the well - where they are continuously exposed to producing fluids. Potential for dissolution of iron bearing species originating from ceramic proppants and the risk of FeS scale formation is currently not known. This presented paper investigates stability of bauxite based ceramic proppants in aqueous H_2S and their ability to form FeS scale, compared to a typical shale core sample.

Experimental Setup

The current study evaluates and compares dissolution kinetics of iron bearing formation and iron containing proppants in aqueous H_2S acid solution. The study uses X-ray diffraction (XRD) to qualify and quantify Fe containing crystallite forms and inductively coupled plasma optical emission spectroscopy (ICP-OES) analysis to quantify their dissolution. Scanning Electron Microscopy (SEM) is used to evaluate surface morphology changes associated with iron dissolution and iron sulfide scale deposition.

Baseline sample analysis

The study investigates chemical reactivity of three different types of proppant sample: LWP (Lightweight Proppant), IDP (Intermediate Strength Proppant) and HSP (High Strength Proppant). All proppant samples used in the study utilize bauxite as their starting raw material source. Core sample used in the study originates from Haynesville shale formation. An x-ray diffraction machine, PANalytical X'Pert Pro, measures phase composition of all used samples by utilizing internal standard reitveld XRD method for analysis. Table 1 lists phase composition of used proppant samples, while Table 2 shows phase composition of a used Haynesville core sample.

Generation of aqueous H_2S solution

The study measures reactivity and dissolution kinetics of samples by subjecting them to aqueous H_2S solution for seven days (168 hours) under ambient temperature (25+/-2ºC) and pressure conditions.

Hydrogen sulfide used in the current study is prepared by reacting ferrous sulfide (FeS) with hydrochloric acid (HCl) in a Kipp generator:

$$FeS + 2\,HCl \rightarrow FeCl_2 + H_2S \qquad (1)$$

Figure 1 exhibits a schematic of the corrosion testing apparatus used in the study. H_2S is a highly toxic and flammable gas. H_2S is also heavier than air and accumulates in low-lying unventilated areas, so efficient operation of fume hoods is critical for personnel safety during these experiments. As shown in Figure 1, H_2S is formed and absorbed in the first beaker where it creates a saturated H_2S solution. The second beaker collects any excess H_2S generated but not absorbed in the first beaker. Neutralization of H_2S by sodium hydroxide solution in the third beaker ensures H_2S does not leave the system.

Theoretically, a saturated solution of H_2S in water has a concentration of approximately 0.10 M. The pH of this solution can be calculated - from Eq. (2) and (3) with the given dissociation constant ($K_{a1} = 9.1x10^{-8}$, $K_{a2} = 1.3x10^{-13}$ mol L^{-1} respectively). As the second dissociation constant is very small, the concentration of H_3O^+ is obtained from the first dissociation constant. The calculated pH value for this saturated solution of H_2S is 4.02. The measured pH of the prepared aqueous H_2S acid is 4.5, which agrees with the theoretical value.

$$H_2S + H_2O \rightarrow H_3O^+ + HS^- \qquad (2)$$
$$HS^- + H_2O \rightarrow H_3O^+ + S^{2-} \qquad (3)$$

Analysis of samples post acid exposure

All tested samples are filtered and dried post acid exposure. pH analysis and inductively coupled plasma optical emission spectroscopy (ICP-OES, Agilent, VARIAN, 720-ES) measures the amount of dissolved particles present in the aqueous H_2S. Microstructure analysis is performed using a scanning electron microscope (SEM, FEI, NOVA nano 230) on polished cross sections and surfaces of both original and acid corroded

ceramic proppant samples and core samples. Compositional mapping is performed using energy dispersive spectroscopy (EDS, EDAX, Apollo 10).

Results

Reaction between Ceramic Proppant and Aqueous H_2S Solution

Figure 2 shows SEM surface analysis of LWP, IDP, HSP ceramic proppant before and after acid exposure. SEM analysis does not show evidence of any Fe precipitation on proppant surfaces despite the fact that Fe containing particles are available, as shown by EDS results.

Figure 3 shows x-ray diffraction patterns of ceramic proppant before and after acid exposure. XRD analysis results confirm EDS analysis. XRD analysis conducted before acid exposure detects Fe in the form of pseudobrookite, $FeAlTiO_5$ compound. This same crystalline form is present after acid exposure and neither pyrite (FeS_2) nor troilite (FeS) are present. This implies that pseudobrookite is a stable crystalline form resistant to H_2S acid attack. A pH analysis of used acid shows a constant value of 4.5. During the experiments, the solution of hydrogen sulfide in water remains clear without turning cloudy over time. This indicates lack of elemental sulfur precipitation, i.e. lack of reaction of hydrogen sulfide with the oxygen in D.I. water. ICP analysis comparison of fresh and spent H_2S acid also does not show presence of any Fe containing species, further confirming chemical stability of the tested proppants. During testing sample mass was recorded; comparison of proppant sample mass pre and post acid exposure reveals no mass loss/gain associated with proppant dissolution or precipitation of solids on proppant surfaces.

Reaction between Shale Core and Aqueous H_2S Solution

Figure 4 shows appearance of a Haynesville shale core sample before H_2S exposure. The shale core sample is not homogeneous and contains veins in the middle section of the sample. SEM and EDS analysis reveals that these veins contain sodium (Na), magnesium (Mg), aluminum (Al), silicon (Si), potassium (K), calcium (Ca), and iron (Fe) elements.

Figure 5 shows the appearance of the shale core sample after H_2S exposure. Exposing the shale sample to aqueous H_2S acid changes the color of the veins into light yellow. Presence of yellow precipitates is associated with deposition of sulfur containing minerals on the rock caused by reaction with H_2S. Figure 6 shows SEM with EDS analysis of the shale sample after H_2S exposure. Deposited sulfur element is found across this vein and is accompanied by the presence of elemental Fe indicating possible iron sulfide precipitation.

XRD analysis further confirms SEM and EDS results. Figure 7 shows the diffraction pattern of the core sample post acid exposure. Pyrite (FeS_2) peak can be detected among crystallized peaks, indicating the formation of sulfide scale. Furthermore, XRD analysis of core samples post acid exposure reveal a lack of the muscovite phase, originally detected in the pristine core sample.

The pH value of the spent H_2S acid is 8.8. This pH value is higher than 4.5 measured in H_2S before core exposure. Acid appearance is also different. While original H_2S is clear and transparent in color, after core exposure acid color is yellow. ICP analysis of spent acid detects many metal ions, such as calcium (Ca2+), potassium (K+), and sodium (Na+).

Summary and Implications

Analytical analysis of three different types of bauxite based proppants, and shale core reveal all samples contain iron bearing crystalline compounds. However, results show that dissolution kinetics of shale core and proppant samples are very different. Iron containing compounds in all ceramic proppants tested in this study demonstrate high stability in aqueous H_2S acid solution. None of the analytical techniques used are able to detect dissolution of iron or FeS precipitation. On the other hand, the iron bearing shale core sample shows high reactivity with aqueous H_2S resulting in both dissolution of shale core as well as precipitation of FeS scale. Since the dissolution of Fe containing minerals in shale is much faster than that seen for proppants, any scale formation observed during the lifetime of the well , points to the primary source of the Fe as originating e either from formation rock or steel piping. Results shown in this study suggest that bauxite based proppants are not a significant contributor to FeS scale formation and can therefore be safely used in sour wells.

Acknowledgements

The authors appreciate the support and permission of Saint-Gobain Proppants to conduct this research and to publish the results.

References Cited

Leal, J., H.A. Nasr-El-Din, C. Franco, F. Garzon, H.M. Marri, S.A. Aqeel, and G. Izquierdo, 2007, A systematic approach to remove iron sulphide scale: a case history: SPE 105607, Society of Petroleum Engineers. doi:10.2118/105607-MS.

Lusk, D., M. Gupta, K. Boinapally, and Y. Cao, 2008, Armoured against corrosion: Hydrocarb. Eng., v. 13, p. 115–118.

Nalli, K., 2010, Corrosion and its mitigation in the oil and gas industry. An overview: PM-Pipeliner Report, Jan-Mar, 2010, p. 10-16.

Nasr-EI-Din, H.A., and A.Y. AI-Humaidan, 2001, Iron Sulfide Scale: Formation, Removal and Prevention: SPE 68315, Society of Petroleum Engineers. doi:10.2118/68315-MS.

Nasr-EI-Din, H.A., A.Y. AI-Humaidan, B.A. Fadhel, and R. Saleh, 2000a, Effect of acid additives on the efficiency of dissolving iron sulfide scale: CORROSION 2000, 26-31 March, Orlando, Florida.

Nasr-El-Din, H.A., B.A. Fadhel, A.Y. Al-Humaidan, W.W. Frenier, and D. Hill, 2000b, An Experimental Study of Removing Iron Sulfide Scale from Well Tubulars: SPE 60205, Society of Petroleum Engineers. doi:10.2118/60205-MS.

Nasr-El-Din, H.A., A.Y. Al-Humaidan, B.A. Fadhel, W.W. Frenier, and D. Hill, 2000c, Investigation of sulfide scavengers in well-acidizing fluids: SPE 80289, Society of Petroleum Engineers. doi:10.2118/80289-PA.

Nasr-El-Din, H.A., M. Zabihi, S.K. Kelkar, and M. Samuel, 2007, Development and field application of a new hydrogen sulfide scavenger for acidizing sour-water injectors: SPE 106442, Society of Petroleum Engineers. doi:10.2118/106442-MS.

Oyelami, B.O., and A.A. Asere, 2011, Mathematical modelling: An application to corrosion in a petroleum industry: NMC Proceedings Workshop on Environment, National Mathematical Centre, Abuja, Nigeria.

Tuttle, R.N., 1987, Corrosion in oil and gas production: J. of Petrol. Technol., v. 39, p. 756–762.

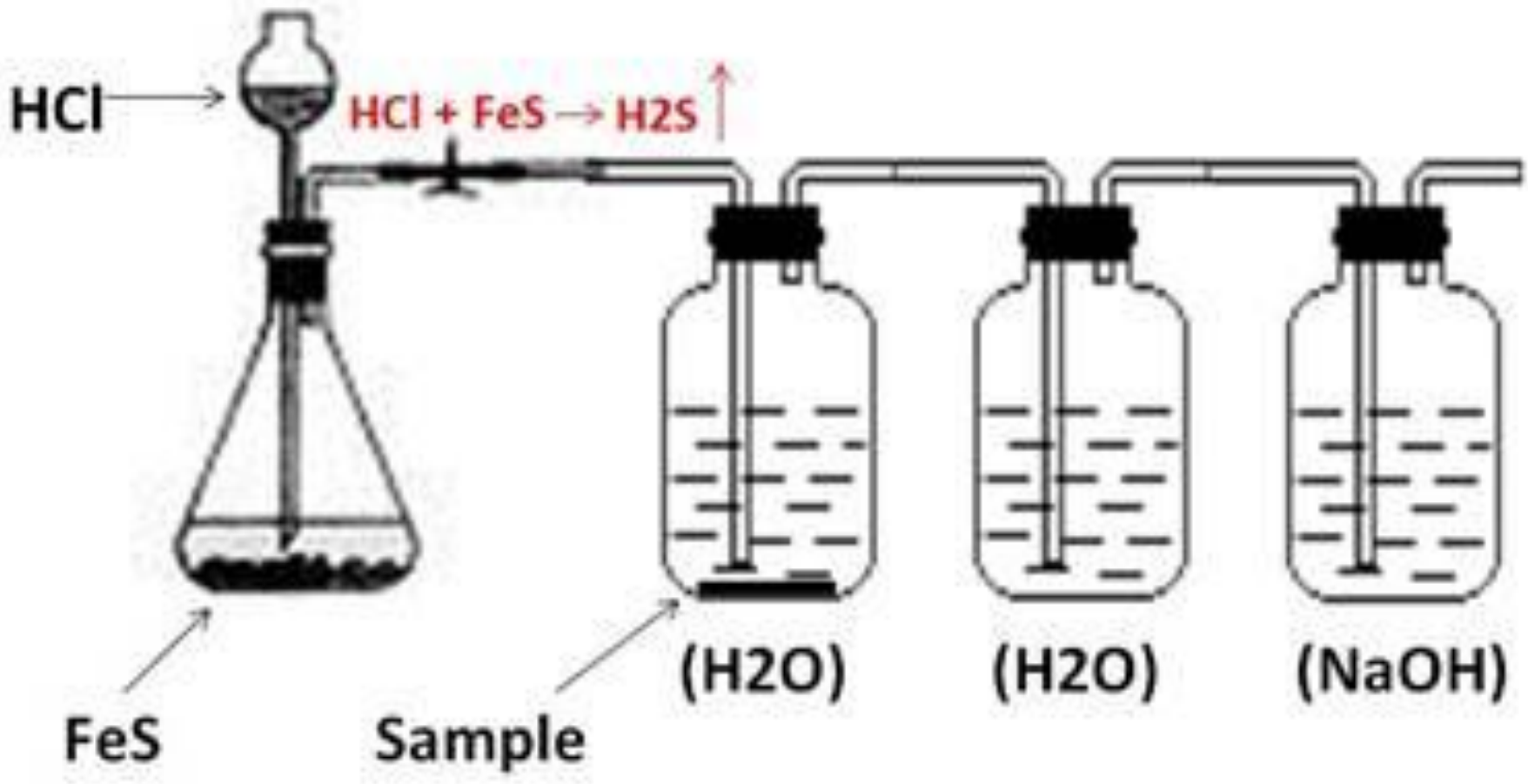

Figure 1. Schematic of H_2S generator and sample reactor.

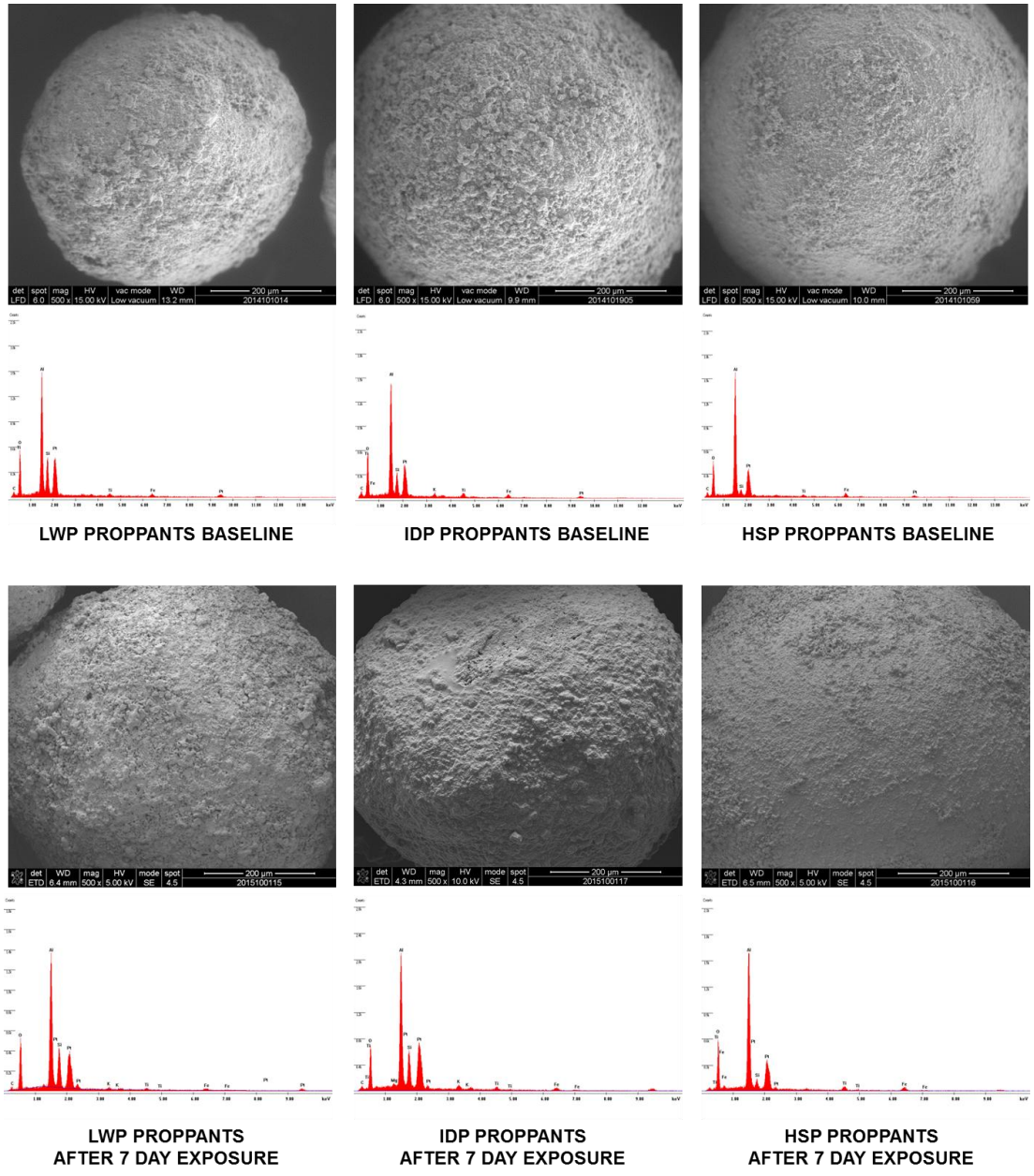

Figure 2. Scanning electron micrographs of LWP, IDP, and HSP proppants surface before and after exposure to aqueous H_2S solution for seven days (168 hours) under ambient temperature (25+/-2ºC) and pressure conditions

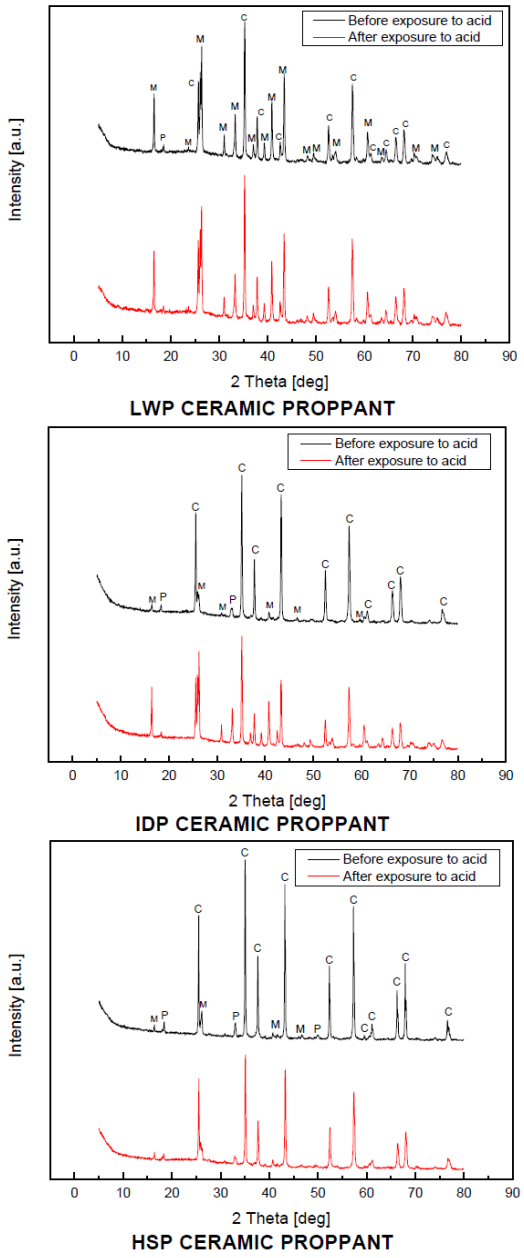

Figure 3. X-ray diffraction patterns of LWP, IDP, and HSP proppants before and after exposure to aqueous H_2S. Labels on the XRD pattern refer to mullite (M), pseudobrookite (P), and corundum (C).

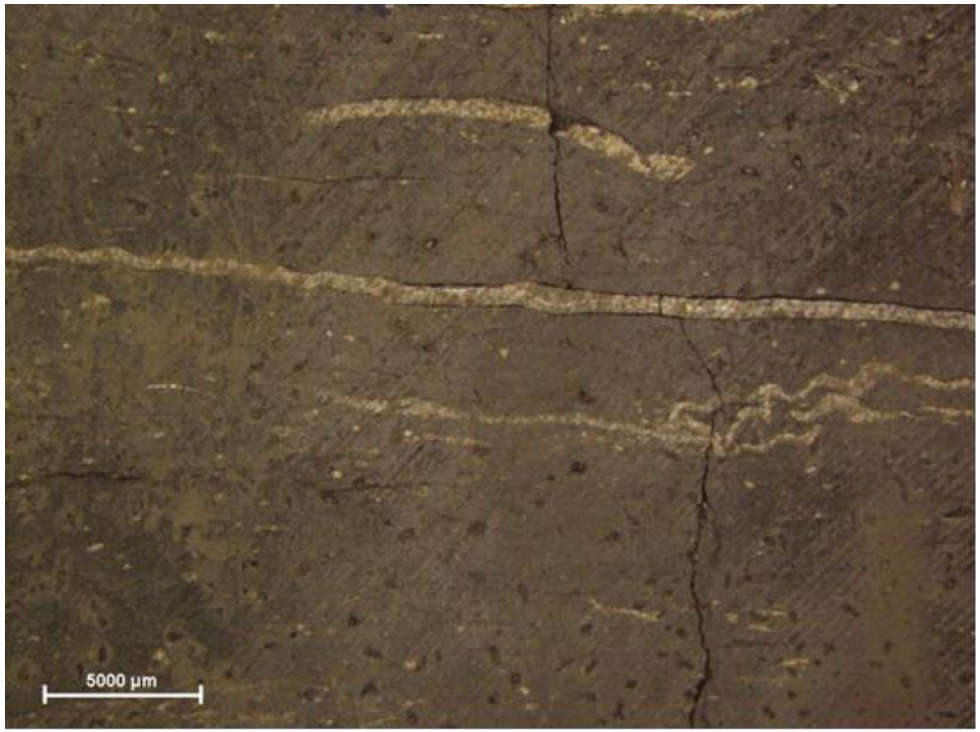

SHALE CORE BASELINE

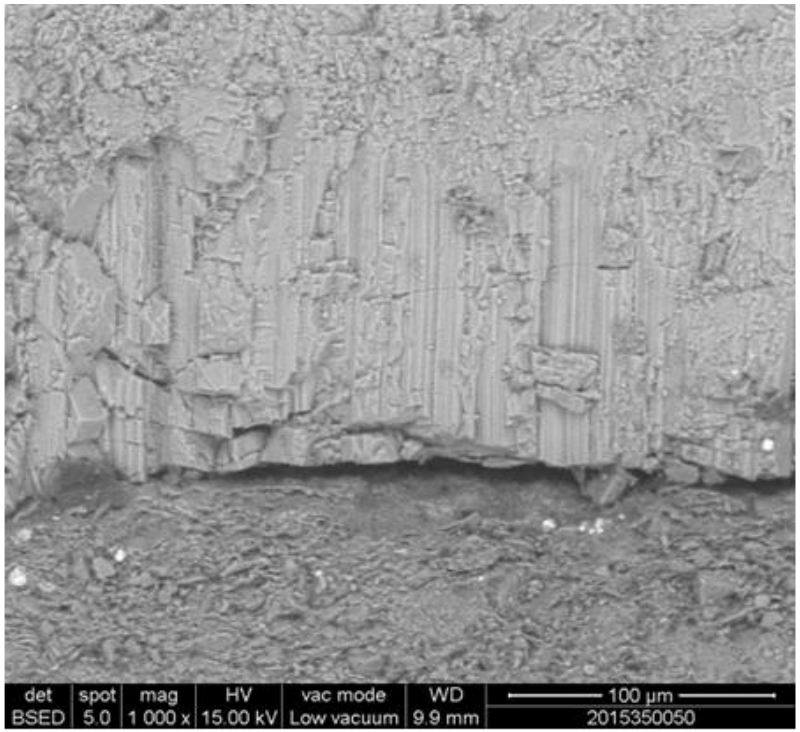

SHALE CORE BASELINE

Figure 4. Optical and scanning electron micrographs of core sample surface.

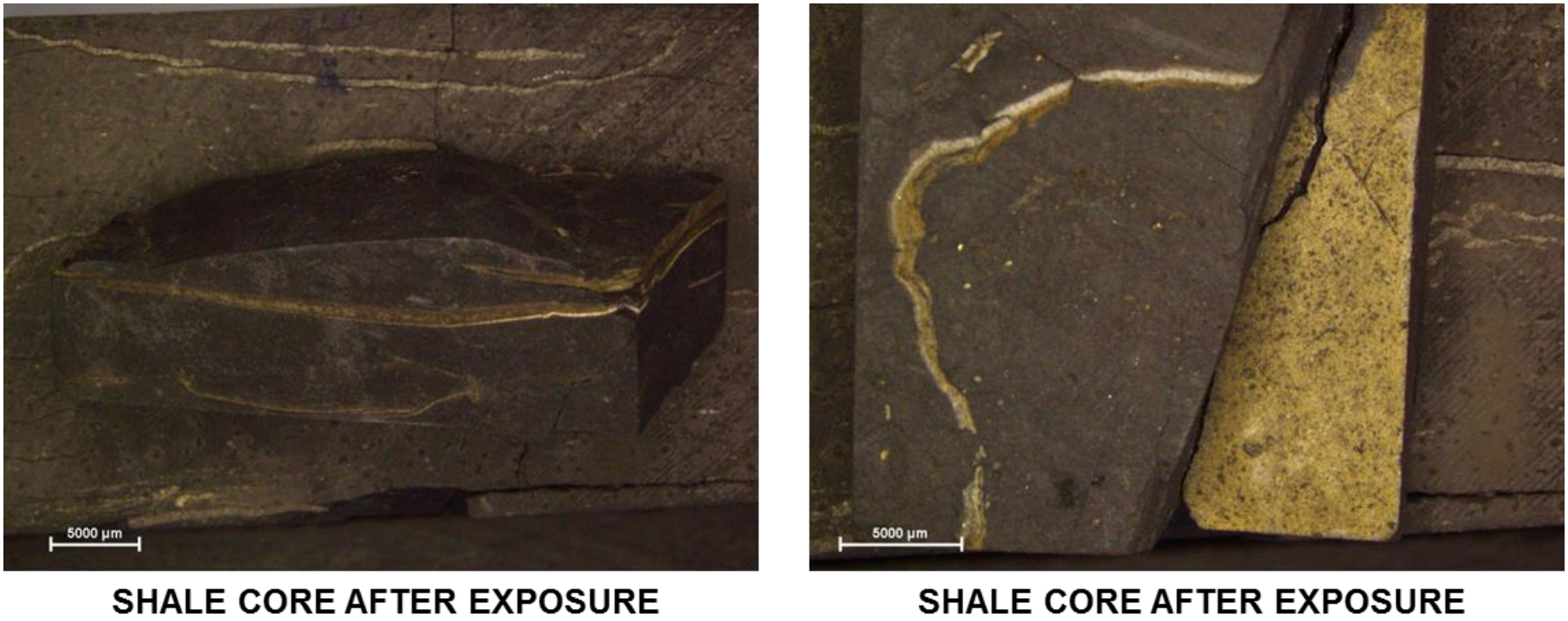

Figure 5. Stereoscopic images of core sample surface post exposure to H_2S.

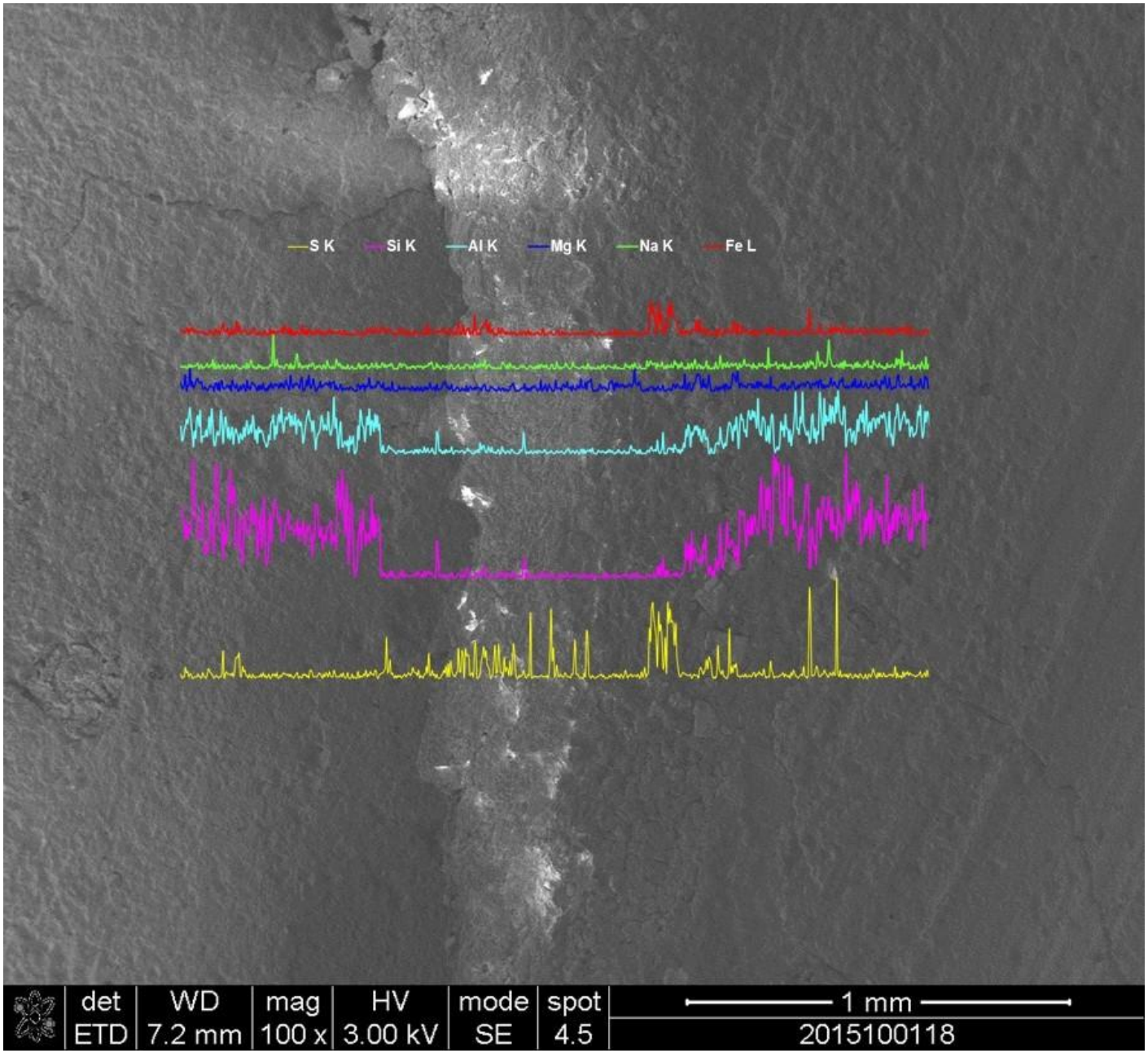

Figure 6. Scanning electron micrograph of core sample after exposure to aqueous H_2S acid with EDS line scanning analysis.

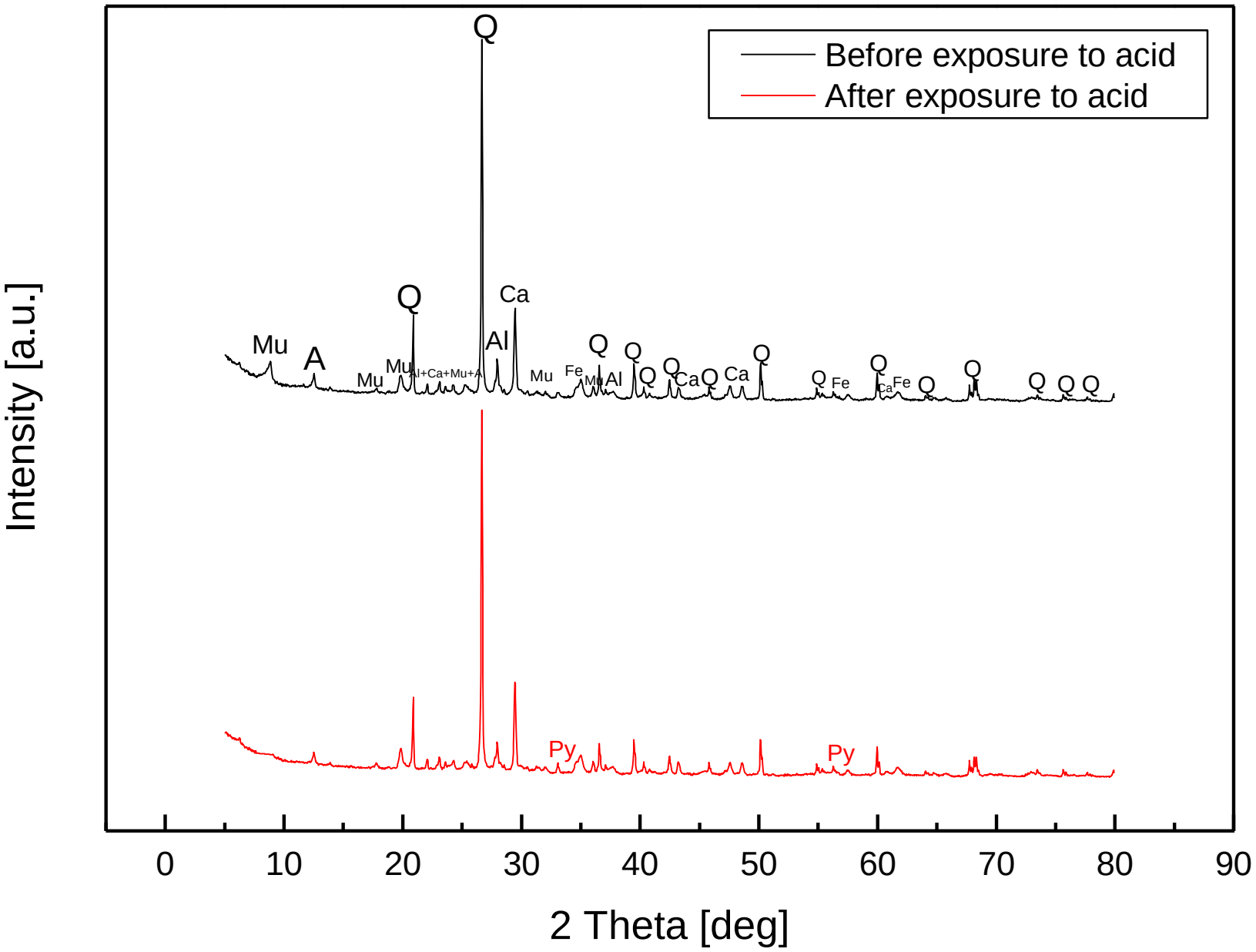

Figure 7. X-ray diffraction patterns of shale core sample before and after exposure to aqueous H_2S. Labels on the XRD pattern refer to muscovite (Mu), albite (Al), amesite (Am), quartz (Q), calcium carbonate (Ca), iron oxide (Fe), and pyrite (Py) respectively.

Phase	LWP	IDP	HSP
Corundum (Al_2O_3)	30.8	59.0	74.7
Mullite ($Al_6Si_2O_{13}$)	36.1	4.9	3.9
Pseudobrookite $FeAlTiO_5$	1.8	3.2	5.4
Amorphous	31.3	32.9	16.0

Table 1. Composition of HSP, IDP, and LWP.

Phases	Shale Core
Quartz SiO_2	27.5
Calcium Carbonate $CaCO_3$	14.8
Iron Oxide Fe_3O_4	1.2
Muscovite $KAl_2Si_3AlO_{10}(OH)_2$	22.8
Amesite $(Mg_2Al)(AlSiO_5(OH)_4)$	3.9
Albite Calcian Low $(Na_{0.84}Ca_{0.16})Al_{1.16}Si_{2.84}O_8$	4.2
Amorphous	25.0

Table 2. Composition of shale core sample.